Australian Journal of Basic and Applied Sciences, 6(9): 683-692, 2012
ISSN 1991-8178

Failure Load of Composite Single-Lap Bolting Joint Under Traction Force and Bending Moment

Esmaeil Ghanbari, Onur Sayman, Mustafa Ozen, Yusuf Arman

Dokuz Eylül University, Izmir, Turkey.

Abstract: The main objective of this paper is to investigate the behavior of single-lap joints in glass fiber reinforced epoxy (GFRE) composites under tension and pure bending loading conditions, with a constant W/D ratio (3) and variable the E/D ratios (3, 4, 5) and tightening torque values (0, 3 and 6 Nm). Bending properties were determined using four-point bending test. The experimental results show that in the tension tests, with increasing E/D ratio and tightening torque, the value of failure bearing stress increased. And in the bending tests, it is seen that atzero torque, with the increase of the E/D ratio, the bending strength value increases, but this increase is small at T=3, 6 Nm torques. And in these tests, the joint failed at the center, near the bolt, because of the excessive delaminations on the compressive side.

Key words: Failure load, Single-lap joint, Composite laminate, Four point bending.

INTRODUCTION

The use of composite materials in structural components of mechanical and civil applications has grown steadily in recent years. Today, many composite parts are made out of different orientations of prepreg tapes and are being used extensively in applications where a joint is required. In composite structures, three types of joints are commonly used, namely, mechanically fastened joints, adhesively bonded joints, and hybrid mechanically fastened/adhesively bonded joints. Bolted joints are still the dominant fastening mechanisms used in joining of primary structural parts made from advanced composites. Mechanical fasteners offer the advantage of being able to be removed without destroying the structure and they are not sensitive to surface preparation, service temperature, or humidity. The procedure for designing mechanically fastened joints in composite materials is predominately based on experimental data and the analytical models are largely empirical in nature. The selection of appropriate or optimum geometric parameters and materials are essential in order to achieve the structural integrity and reliability in composite structures, since bolted joints in composites fail at loads that are not predicted by either perfectly elastic or perfectly plastic assumptions. Any joint in a composite structure, if not designed appropriately, may act as a damage initiation point and may lead to failure of the component at that location.

A major goal of bolted joint research is to determine the effect of various bolting parameters on the bearing strength of the joint .These parameters include: (a) joint geometry (specimen width, end distance, and hole diameter); (b) joint configuration (single over lap, double lap, single bolt, single bolt row, or multi-bolt row); (c) loading condition (tension, compression or combined static and/or fatigue loading); (d) fastening parameters (bolt/hole clearance, bolt/washer clearance, tightening torque or clamping force, washer size, and presence of countersink); and (e) material parameters (stacking sequence, fiber shape, matrix type, fiber volume fraction). In summary, the joints would be expected to eventually fail in a variety of modes; namely, net-tension, shearing-out, and bearing Fig 1. In terms of structural design, bearing failure preferably occurs as a combination of these three modes, in view of the stability of the failure process. However, bearing failure is a local compressive failure mode due to contact and frictional forces acting on the surface of the hole. This fracture process is very complicated and is influenced by many parameters, including washer dimension and lateral clamping force.

Crews (1981) conducted static and fatigue tests under bolt-bearing loads for a range of bolt clamp-up torques. He reported that bolt clamp-up force exerts a significant effect on both static strength and fatigue limit. Eriksson (1990) has shown that bearing strength is influenced by several important parameters, including lateral constraint conditions and ply orientations. Wang *et al*. (1996) used bearing response and bearing strength of bolted joints to examine the bearing failure mechanism as a function of clamping pressure. In their work, a pin-loaded bearing (without lateral clamping) test and a bolted bearing (with lateral clamping) test were conducted to evaluate the bearing damage. Wu and Sun (1998) investigated the behavior of pin-contact failure of composite laminates and found that fiber micro-buckling in the 0-deg plies of the laminate plays an important role in the initiation of bearing damage. Camanho *et al*. (1998) carried out a detailed experimental investigation for three basic failure modes of a joint, and their results show that the main mechanism of bearing failure is accumulated as delamination damage.

Khashaba (2006) showed that there is an optimum washer size of for constant clamping force, which balances the amount of area constrained against the amount of clamping pressure produced. Laminate lay-up

Corresponding Author: Esmaeil Ghanbari, Dokuz Eylül University, Izmir, Turkey.

also affects joint performance and it is strongly related to the type of failure mode (Alaattin A., 2003; 2004). Quinn (1977) found that laminates with 90° layers near the surface of the laminate produce higher bearing strengths (a 90° lamina has fibres perpendicular to the direction of loading). The higher bearing strengths were attributed to lower interlaminar stresses due to the outer 90° layers.

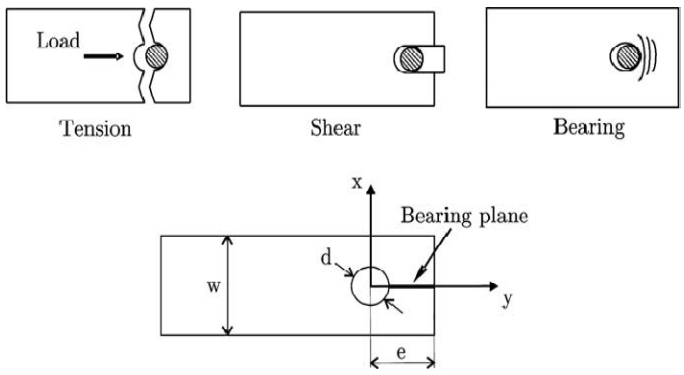

Fig. 1: Failure modes of composites structural.

Aktas and Dirikolu (2003) investigated a pin loaded carbon epoxy composite laminate with different stacking sequences in order to determine its safe and maximum bearing strengths, experimentally. Tong (2000) reported an experimental investigation on the effect of non-uniform bolt-to-washer radial clearance on bearing failure of bolted joints under different clamping forces with various lateral constraints. Experimental results were also used to validate an existing model. Two extreme diametral fit positions, with a positive or negative bolt hole-to-washer clearance, were also considered.

Chang *et al*. (1984) developed a method to size laminates containing one or more pin loaded holes. They also showed how the design parameters, number of holes, hole diameter and hole position can be found to predict the maximum failure load. They also predicted the failure strength and failure modes by Yamada–Sun failure criteria in one and two-pin holes by using the finite element method. Ryu *et al*. (2007) have examined failure load using linear finite analyses in mechanically fastened composite joints and compared their results with experiments. Sayman and Ahishali (2008), have carried out an experimental failure analysis on mechanically fastened joints in composite laminate under 2.5 and 5 Nm preload moments. Kweon *et al*. (2007) conducted a two-dimensional progressive failure analysis to predict the failure loads and modes of uni-directional-fabric laminated composite joints under pin loading by applying a two-dimensional progressive damage analysis program (ACOS-J). They also studied the effect of various failure criteria and have shown that a finite element analysis based on the combined Yamada–Sun and Tsai–Wu criteria accurately predicted the failure loads of the composite laminated joints. Karakuzu *et al*. (2008) studied the effects of geometrical parameters on the failure loads and failure modes in woven glass vinyl ester composite plates with two serial and parallel pin loaded holes. They conducted experiments and numerical analysis using LUSAS by employing Hashin failure criterion. They concluded that ultimate load capacity depends on E/D, S/D and P/D ratios.

Camanho and Matthews (1999) have developed a 3D finite element model to predict damage progression and strength of mechanically fastened joints in carbon-fiber reinforced plastics. To predict the failure mode, Hashin failure criteria have been used and compared with the experimental results. Sayman *et al*. (2007) studied the characterization of the bearing strengths of mechanically fastened joints with single bolt in glass–epoxy laminated composite plates experimentally.

In the present study, the effects of tightening torque and edge distance-to-hole diameter (E/D) on the strength of bolted joint in single-lap joints with tabs that are bonded to the ends of the test specimens and fabricated from glass fiber reinforced epoxy composite materials, are investigated experimentally. The composites have a stacking sequence of $[0/45/30/-30]_{2s}$ and are subjected to the traction and four point bending moment tests. The mechanical properties of the composite laminate (tension, compression, and shear) are determined experimentally.

2. Experimental Study:

2.1. Specimen Preparation:

The angle-ply $[0/45/30/-30]_{2s}$ glass fiber reinforced epoxy (GFRE) composite laminates were fabricated in Izorel Firm in Izmir. All composite laminates lay-up were covered with a release film to prevent the lay-up from bonding to the mold surface. After that, resin impregnated fibers were placed in the mold for curing. The press generated the temperature and pressure required for curing. The mould was closed down to give the nominal thickness. The glass fiber/epoxy material was cured at 120^0C under a pressure of 0.2 MPa. This temperature was

held constant for 4 h for the first phase. Next, the temperature was decreased to 100^0C and held constant for 2 h for the second phase under the same pressure of 0.2 MPa. Later, the laminates were cooled to room temperature. Finally, the laminated plate was removed from the press and cut to specimen dimensions. The final thickness of the specimens had an average thickness of 3.82 mm. Fiber volume fraction (V_f) was determined experimentally so that the composite specimen was fired in an electrical oven, then, the volume fraction of the glass fibers was calculated as 38%.

2.2. The Mechanical Properties:

A series of ASTM standard tests were carried out on different orientations of GFRE composites using universal testing machine, in this study all the mechanical tests were performed by using SHIMATZU tensile test machine. The crosshead speed of the loading member in compression, tension, in-plane shear, bolted joint, and four point bending tests was 1 mm/min. Three specimens were tested for each test shape and the mean values were used for drawing the different relationships. Two of these specimens were chosen for measuring the strains in tension and in-plane shear tests using a digital strain meter TDS-530 that is described in the following sections.

2.2.1. Tension Test:

Tensile properties of angle-ply $[0/45/30/-30]_{2s}$ composites were determined experimentally. Longitudinal Young's modulus E_1, longitudinal tensile strengths X_t, Poisson's ratio v_{12}, transverse Young's modulus E_2, and transverse tensile strengths Y_t were measured by using longitudinal and transverse $[0]_8$unidirectional composite specimens in accordance with the ASTM D3039-76 standard. The test specimens were loaded until failure occurred in the axial and transverse directions. Young's moduli of E_1 and E_2 were calculated by the tensile machine by using two digital cameras which were mounted on the machine for measuring the variations in longitudinal axis of the machine using the initial slope of the stress–strain curves for these calculations. The tensile strengths of the unidirectional composite plates, X_t andY_t, were determined by dividing the failure load to the cross sectional area of the longitudinal and transverse specimens, respectively. Poisson's ratio v_{12} was measured using the strain gages that bonded at the center of the test specimen. The dimensions of the test specimen are shown in Fig.2.

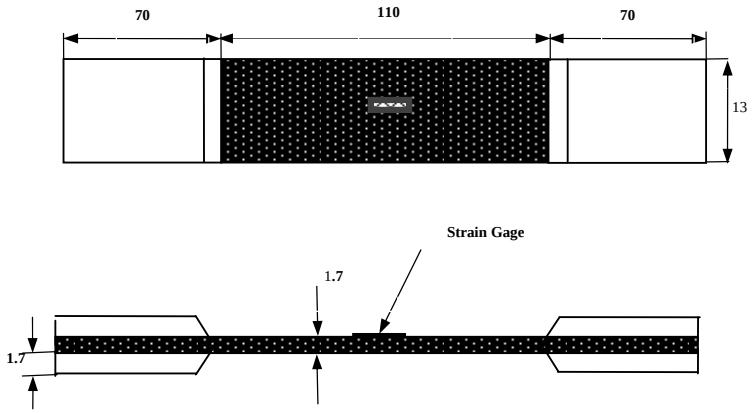

Fig. 2: Dimension of tensile test specimen.

2.2.2. Compression Test:

The compression properties of the composite laminates were determined experimentally using the Illinois Institute of Technology Research Institute (IITRI) compression test fixture. The compression test specimens with 140 mm length were prepared according to ASTM D3410 standard. The width was taken as 13 and 25 mm for the longitudinal and transverse specimens, respectively. The longitudinal and transverse compressive strengths, X_c and Y_c, were obtained by dividing the failure loads to the cross-sectional area of the specimens. The dimensions of the compression test specimens are shown in Fig. 3.

2.2.3. In-Plane Shear Test:

The in-plane shear properties of the composite laminate were determined using the V-notch beam method by using Arcan test fixture as shown in Fig. 4. The specimens with 90^0 notches were prepared from $[0]_8$unidirectional glass/epoxy laminated composites according to ASTM D5379. Tensile force was applied to Arcan test fixture until failure occurred. The in-plane shear strength S_{12} was calculated by:

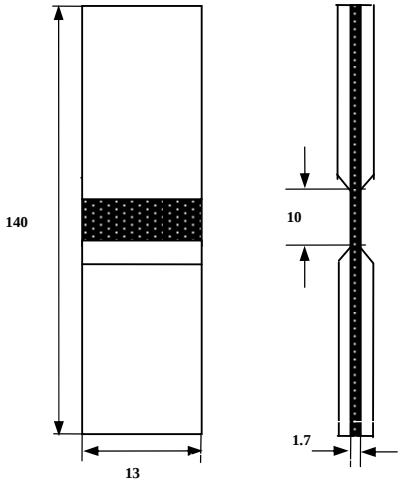

Fig. 3: Dimension of compressive test specimen.

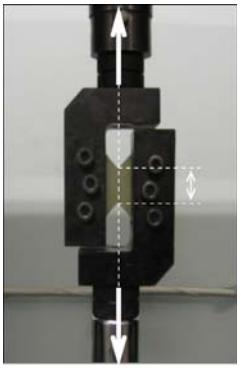

Fig. 4: Arcan test fixture.

$$S_{12} = \frac{P_{\max}}{wt} \tag{1}$$

Where P_{max} is the failure load, w is the width of the specimen at notch location and t is the specimen thickness. Shear modulus G_{12} was measured by using two strain-gages located at the center of the notched section at 45^0 and -45^0 to the loading direction. Shear stress τ_{12} was obtained by using Eq (1). The shear modulus was calculated by using the following equation

$$G_{12} = \frac{\tau_{12}}{(\varepsilon_{45^0} - \varepsilon_{-45^0})} \tag{2}$$

The experimental results of tensile, and compressive, and in-plane shear tests are illustrated in Table 1.

Table 1: Mechanical properties of glass-epoxy laminated composite plate

E_1 (GPa)	E_2 (GPa)	G_{12} (GPa)	ν_{12}	X_t (MPa)	Y_t (MPa)	X_c (MPa)	Y_c (MPa)	S (MPa)	V_f (%)
31.0	10.5	4.8	0.27	821.0	78.0	377.0	137.0	62.0	38

2.2.4. Bolted Joint Test:

The strength of bolted joints with various values of tightening torque (T = 0, 3, and 6 Nm), constant width-to-diameter ratio (W/D=3) and the edge distance-to-hole diameter ratio (E/D= 3, 4, 5) in tension and four point bending, was determined, experimentally. The dimensions of the bolted joint specimen according to ASTM

D5961 standard is shown in Fig. 5. (a), (b). To eliminate the secondary bending effects in tensile loading and to have symmetric geometry in the bending the tabs were bonded to the ends of the test specimen.

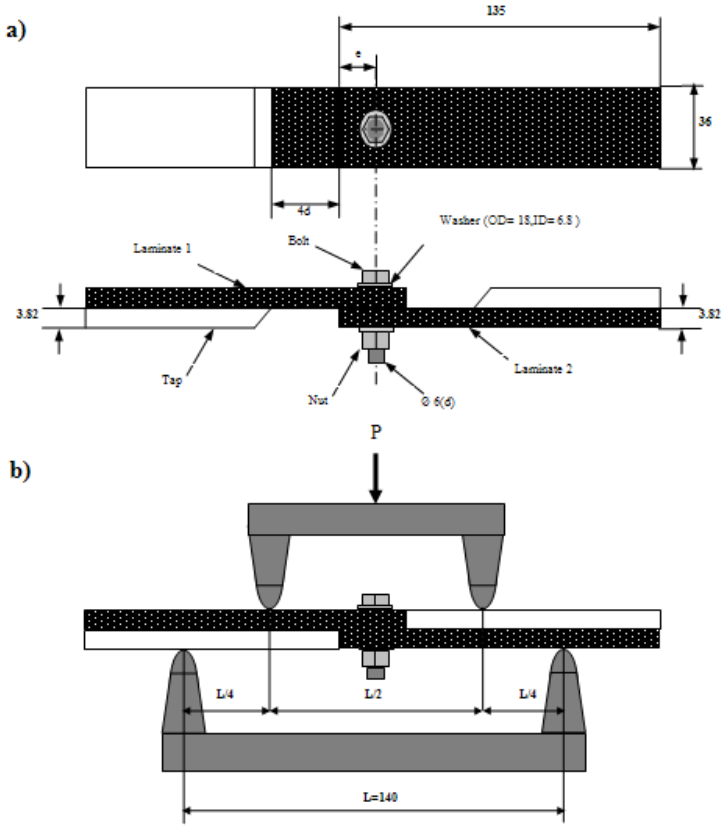

Fig. 5: Dimension of bolted joint (a) tensile test (b) four point bending.

RESULTS AND DISCUSSION

3.1. Effects of E/D Ratio and Tightening Torques:

In this section, 0, 3 and 6 Nm tightening torques were applied the test specimens before loading and the effects of these torques were examined. Thus, the effects of the increasing tightening torque on failure behavior and bearing strength at tension and bending moment under four point bending tests were investigated. The bearing strength was calculated as:

$$\sigma_b = \frac{P_{\max}}{Dt} \tag{3}$$

Where $P_{max}$is the maximum failure load, D is the diameter of the hole and t is thickness of the specimens.

Fig 6. shows the influence of tightening torque on the behavior of bearing failure of bolted joint specimens with constant W/D = 3 and variable E/D =3-5 in the tensile test. The results in this figure indicate that, the bearing strength of the bolted joint increases by increasing the tightening torque. Therefore, the tensile loads under 6 Nm tightening torques are higher than those under 0 and 3 Nm tightening torques, in general. In addition, the axial failure loads under 3 and 6 Nm tightening torques are usually calculated very close to each other. Nevertheless, the failure loads without tightening torque are small in comparison with the other tightening torques. Therefore, it seems that increased values of tightening torques satisfy a strong structure so that the load carrying capacity of the single-lap bolted joint of the fiber reinforced composite plates increases by increasing the tightening torque. Similar behavior was observed in previous publications for bolted joints (Khashaba U. A., 2006; Tong L. 2000; Sayman O, 2011; 2007). But it seems that failure bearing strength decreases or does not change with continuous increase of tightening torque, similar to, that observed by Khashaba (2006).

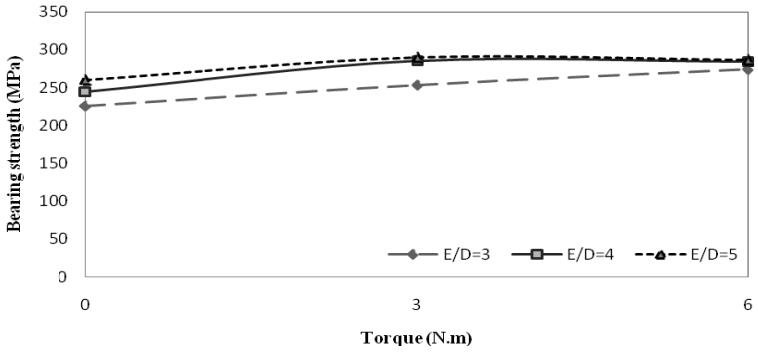

Fig. 6: The effect of E/D and torque on the bearing strength in traction test.

Traction or axial forces versus displacement under T = 0, 3, 6 Nm for E/D=3 are shown in Fig 7. (a). As seen, when the tightening torque increases, the failure load reaches higher values. It is also seen that the net-tension failure mode occurs for E/D=3. Traction forces versus displacement under T=3 Nm for E/D=3-5 are shown in Fig 7. (b). It seems that net-tension failure mode occurs for E/D=3, nevertheless, the bearing failure mode occurs for E/D=4, 5. When E/D increases, the failure mode becomes the bearing mode. The bearing mode is preferred to other modes.

The effect of the E/D ratio on the bearing strength under T=0, 3, 6 Nm tightening torques is shown in Fig 8. As seen, when E/D ratio increases the bearing strength increases gradually. The bearing strength represents a close result under T=3 and 6 Nm tightening torques.

The effect of the tightening torques on the bending moment was investigated by conducting the four point bending moment test. A typical curve is shown in Fig 9. It is seen that when the torque increases, the failure bending moment increases for E/D=3, 4, 5. The ratio of E/D=5 satisfies the highest bending moment. The 3 and 6 Nm torques produce close results for E/D=3, 4, 5.

The influence of E/D ratio on the bending moment for T=0, 3, 6 Nm is shown in Fig 10. It seems that T=3 and 6 Nm tightening torques produce close values for E/D=3-5. Moreover, the bending moment is small when the tightening torque equals to zero, in comparison with the values for T=3 and 6 Nm.

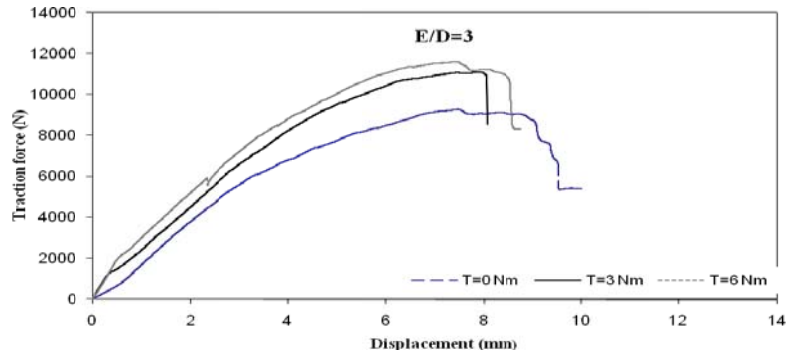

(a)

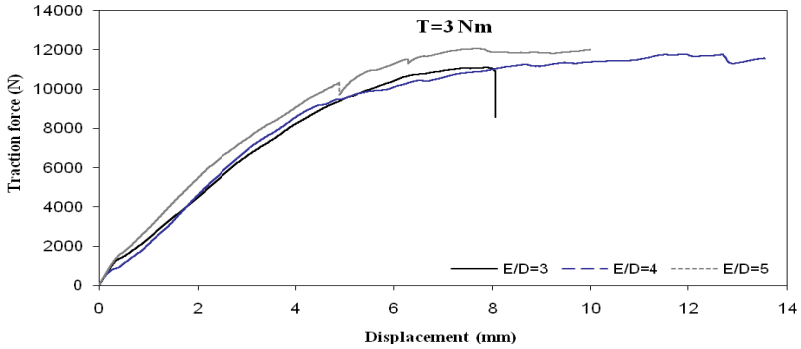

(b)

Fig. 7: Force-displacement curves: a) E/D=3 and tightening torque variable. b) T=3 Nm and E/D variable.

3.2. Failure Modes:

Each test specimen was loaded until the occurrence of the last failure. The general behavior of the composite joint was determined from the load–displacement curves. Two different failure types were observed during the tensile tests of the study: Bearing, net tension and the combination of these modes. The typical load/displacement curves are shown in Fig. 7 (a), (b). for T = 3 and E/D = 3, and the complete failure modes can be seen in Table 2. The failure mode for the bending moment test is the same mode for all, so that, all of the test specimens fail in transverse direction, similar to net-tension, near the bolt hole. The initial failure starts on the surface layers of the compressive side of the specimen. The typical failure bending moment curves are shown in Fig 11. (a), (b). It seems that the failure modes are similar to the net-tension mode. The curves fall down suddenly after failure occurring.

In all of the diagrams after reaching the maximum load, three types of decreasing force values occur:

a) The rapid drop that is the net-tension failure mode. This failure mode occurs for small E/D ratios and tightening torque values. The load decreases suddenly after reaching the ultimate force. Also the tear occurs suddenly in this mode.
b) No rapid drop that is the bearing failure mode. The failure load increases after the first peak and it continues carrying the load. The last failure occurs in large deformations of the bolt. It still carries the load in this case; although, the maximum load is be taken as the ultimate failure load of the specimen. This mode occurs for high E/D ratio and high tightening values.
c) The combination of the above modes. In this case, the load reaches the maximum load and then decreases slowly and again experiences a sudden rapid drop. This mode of failure is the combination of the net-tension and bearing failure modes during loading.

The failure modes of all specimens are given in Table 2.

Table 2: Failure modes and values of the failure load and bearing strength.

E/D	Failure mode	Failure load (N)	Bearing strength (MPa)
T=0 Nm			
3	N	9746	225.60
4	N	10966	253.80
5	B+N	11843	274.10
T=3 Nm			
3	N	10579	244.90
4	B+N	12340	285.60
5	B	12303	284.80
T=6 Nm			
3	N	11215	259.60
4	B+N	12510	289.60
5	B	12360	286.20

N: Net-tension mode, B: Bearing mode.

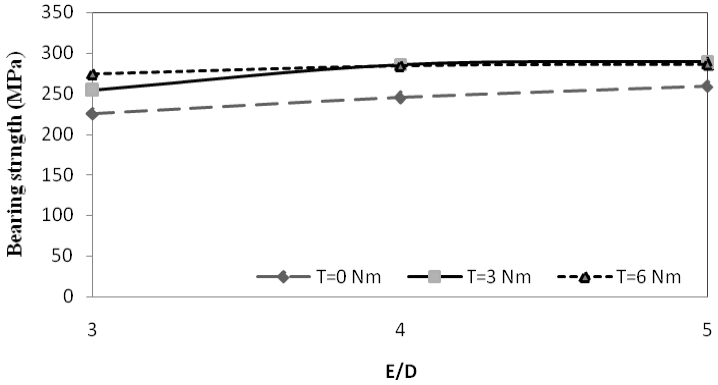

Fig. 8: The effects of E/D ratio on the bearing strength.

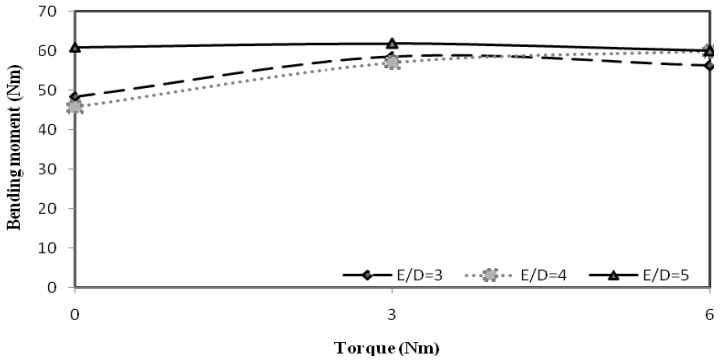

Fig. 9: The effect of tightening torque on the bending moment.

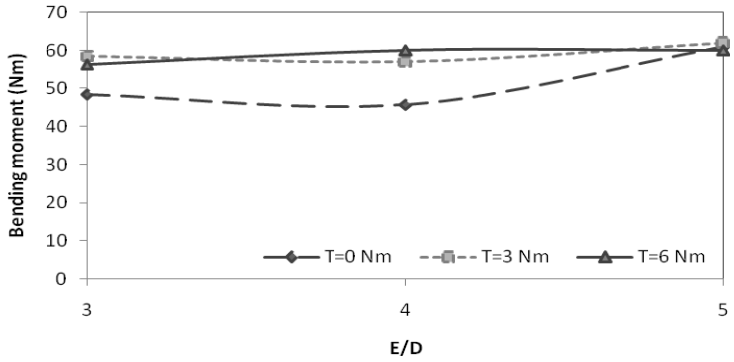

Fig. 10: The effect of E/D ratio on the bending moment.

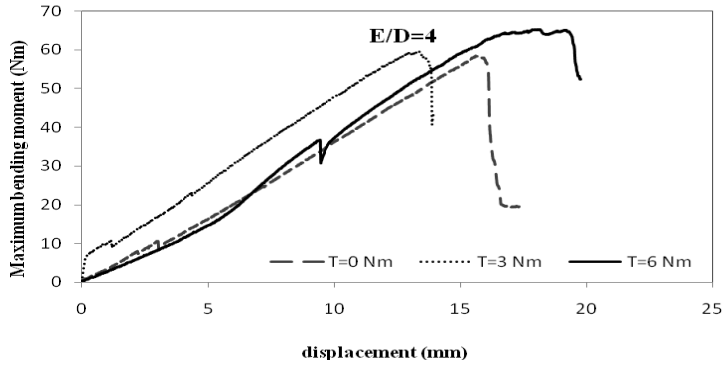

(a)

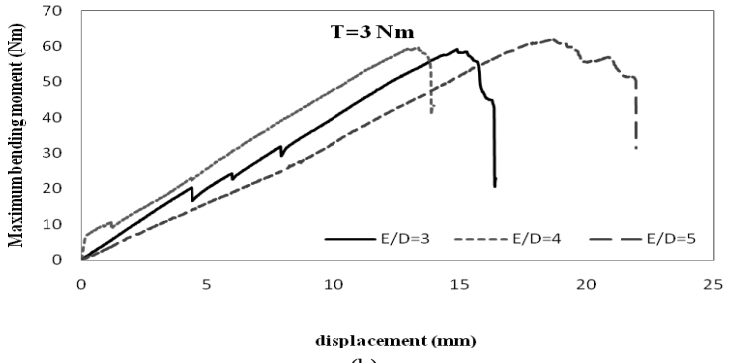

(b)

Fig. 11: The moment and displacement curves: a) E/D=4 and tightening torque variable. b) T=3 Nm and E/D variable.

Conclusions:

The failure of the single-lap joint was examined under axial forces and bending moments. The bending moments were produced by four point bending method. The following results can be concluded from tests:

a) Under axial traction force, the bearing strength increases when E/D ratio and tightening torque values increases.
b) The tabs that bonded to the ends of the specimen eliminate the effects of secondary bending.
c) When the tightening torque increases the maximum bending moment increases
d) The failure load increases considerably for T=0, whereas it increases slightly and gives close results under T=3, 6 Nm bending moments. It is almost linear for E/D=5. As a result of this, the 3 Nm tightening torque will be generally adequate for this joint.
e) Failure bending moment increases when E/D increases without a tightening torque or T=0.
f) In the bending tests, the failure firstly begins on the compressive side and the joint fails at the center near the bolt, because of the excessive delaminations on the compressive side, due to the small strength of X_c.

REFERENCES

Crews, JHJ., 1981. Bolt-bearing fatigue of a graphite/epoxy laminate. In: Kedward KT, editor. Joining of composite materials, ASTM STP 749. American Society for Testing and Materials; pp: 131-44.

Eriksson, I., 1990. On the bearing strength of bolted graphite/epoxy laminates. J Compos Mater, 24: 1264-9.

Wang, HS., CL. Hung, FK. Chang, 1996. Bearing failure of bolted composite joints. Part I: experiments. J Compos Mater, 30(12): 1284-313.

Wu PS., CT. Sun, 1998. Bearing failure in pin contact of composite laminates. AIAA J, 36(11): 2124-9.

Camanho, PP., S. Bowron, FL. Matthews, 1998. Failure mechanisms in bolted CFRP. J ReinfPlast Comp 17: 205-33.

Khashaba, U.A., H.E.M. Sallam, A.E. Al-Shorbagy & M.A. Seif, 2006. Effect of washer size and tightening torque on the performance of bolted joints in composite structures. *Composite Structures*, 73: 310-317.

Alaattin, A. & M.H. Dirikolu, 2003. The effect of stacking sequence of carbon epoxy composite laminates on pinned-joint strength. *Composite Structures*, 62: 107-111.

Alaattin, A. & M.H. Dirikolu, 2004. An experimental and numerical investigation of strength characteristics of carbon-epoxy pinned-joint plates. *Composite Science and Technology*, 64: 1605-1611.

Quinn, W.J. & F.L. Matthews, 1977. The effect of stacking sequence on the pin-bearing strength in glass fibre reinforced plastic. *Journal of composite Materials*, 11: 139-145.

Aktas, A., MH. Dirikolu, 2003. The effect of stacking sequence of carbon epoxy composite laminates on pinned-joint strength. Composite Structeres, 62: 107-11.

Tong, L., 2000. Bearing failure of composite bolted joints with non-uniform bolt-to-washer clearance. Compos Part A: Appl Sci Manufact, 31: 609-15.

Chang, FK., RA. Scott, GS. Springer, 1984. Failure of composite laminates containing pin loaded holes method of solution. J Compos Mater, 18: 255-78.

Ryu, C., J. Choi, J. Kweon, 2007. Failure load prediction of composite joints using linear analysis. J Compos Mater, 41(/7): 865-78.

Sayman, O., M. Ahishali, 2008. Failure analysis of bolted aluminum sandwich composite plates under compressive preload. J ReinfPlast Compos, 27(/1): 69-81.

Kweon, JH., SY. Shin, JH. Choi, 2007. A two-dimensional progressive failure analysis of pinned joints in unidirectional-fabric laminated composites. J Compos Mater, 41: 2083-104.

Karakuzu, R., CR. Caliskan, M. Aktas, BM. Icten, 2008. Failure behavior of laminated composite plates with two serial pin-loaded holes. Compos Struct, 82: 225-34.

Karakuzu, R., N. Taylak, BM. Icten, M. Aktas, 2008. Effects of geometric parameters on failure behavior in laminated composite plates with two parallel pin-loaded holes. Compos Struct, 85: 1-9.

Camanho, PP., FL. Matthews, 1999. A progressive damage model for mechanically fastened joints in composite laminates. J Compos Mater, 33: 2248-80.

Sayman, O., R. Siyahkoc, F. Sen, R. Ozcan, 2007. Experimental determination of bearing strength in fiber reinforced laminated composite bolted-joints under preload. J ReinfPlast Compos, 26: 1051-63.

Pakdil, M., F. Sen, O. Sayman, S. Benli, 2007. The effect of preload on failure response of glassepoxy laminated composite bolted-joints with clearance. J ReinfPlast Compos, 26: 1239-52.

Sen, F., O. Sayman, 2009. Experimental failure analysis of two serial bolted composite plates. J Appl Polym Sci., 113: 502-15.

Choi, JH., CS. Ban, JH. Kwean, 2008. Failure load prediction of a mechanically fastened composite joint subjected to a clamping force. J Compos Mater, 42(14): 1415-29.

Sayman, O., M. Ozen, 2011. Failure loads of mechanical fastened pinned and bolted composite joints with two serial holes. Composites: Part B 42: 264-274.

Sayman, O., S. Kapti, M. Ozen, S. Benli, 2007. Experimental and numerical failure analysis of carbon/epoxy laminated composite joints under different conditions. J ReinfPlast Compos, 26: 1051-63.